

Quantum oscillation beyond the quantum limit in pseudospin Dirac materials

C. M. Wang,^{1,2,3} Hai-Zhou Lu,^{2,3,*} and X. C. Xie^{4,5,6}

¹*Department of Physics, Shanghai Normal University, Shanghai 200234, China*

²*Institute for Quantum Science and Engineering and Department of Physics, Southern University of Science and Technology, Shenzhen 518055, China*

³*Shenzhen Key Laboratory of Quantum Science and Engineering, Shenzhen 518055, China*

⁴*International Center for Quantum Materials, School of Physics, Peking University, Beijing 100871, China*

⁵*CAS Center for Excellence in Topological Quantum Computation, University of Chinese Academy of Sciences, Beijing 100190, China*

⁶*Beijing Academy of Quantum Information Sciences, West Building 3, No. 10, Xibeiwang East Road, Haidian District, Beijing 100193, China*

(Dated: July 20, 2020)

Recently, many unexpected fine structures in electric, magnetic, and thermoelectric responses at extremely magnetic fields in topological materials have attracted tremendous interest. We propose a new mechanism of quantum oscillation beyond the strong-field quantum limit for Dirac fermions. The amplitude of the oscillation is far larger than the usual Shubnikov–de Haas oscillation. The oscillation tends to be periodic in the magnetic field B , instead of $1/B$. The period of the oscillation does not depend on the Fermi energy. These behaviors cannot be described by the famous Lifshitz-Kosevich formula. The oscillation arises from a mechanism that we refer to as the inversion of the lowest Landau level, resulted from the competition between the pseudospin Dirac-type Landau levels and real-spin Zeeman splitting beyond the quantum limit. This inversion gives rise to the oscillation of the Fermi energy and conductivity at extremely large magnetic fields. This mechanism will be useful for understanding the unexpected fine structures observed in the strong-field quantum limit in Dirac materials.

Introduction – In a strong magnetic field, the energy spectrum of non-interacting electrons is quantized into the Landau levels. The spacing and degeneracy of the Landau levels increase with increasing magnetic field, so the Fermi energy (which marks the highest energy the electrons occupy at) crosses the Landau levels one by one, leading to the quantum oscillations of the resistivity (Shubnikov-de Haas) and magnetization (de Haas-van Alphen). In an extremely strong magnetic field the system can enter the quantum limit (QL) in which the carriers occupy only the lowest zeroth Landau level. In the QL, the quantum oscillation is supposed to cease because there is no lower Landau level that allows the Fermi energy to move onto. In the newly discovered 3D topological semimetal [1–12], unexpected oscillation-like fine structures have been reported in the QL and cannot be understood by the theory of quantum oscillation, such as magnetic-tunnelling-induced Weyl node annihilation [13, 14], breakdown of the chiral anomaly [15], log-periodic oscillations [16], forbidden backscattering [17, 18], anomalous thermoelectric effects [19–22], and the magnetic torque and magnetization anomalies [23, 24].

In this Rapid Communication, we propose a theory of quantum oscillation beyond the QL, due to a mechanism that we refer to as the inversion of the lowest Landau level (ILLL), i.e., the lowest Landau band may exchange their positions in energy at a critical magnetic field in topological Dirac materials where only pseudospin is coupled

to momentum. Because usually oscillations are not supposed to happen at the quantum-limit magnetic fields, we refer to them as the quantum oscillations beyond the QL. This inversion does not need the topological band inversion in the absence of magnetic field [25, 26]. This ILLL induced oscillation beyond the QL is absent for Schrödinger electrons even in the presence of Zeeman interaction or spin-orbital coupling [27, 28]. The new quantum oscillation can be measured in the conductivity. This energy spectrum driven mechanism is distinct from the usual Shubnikov-de Haas oscillation (SdHO) in several aspects (Table I). The oscillation due to the ILLL beyond the QL is periodic in the magnetic field B , not in $1/B$ as the SdHO is. The frequency of the oscillation does not depend on the Fermi energy. We use a 2D massless graphene-like Dirac model to illustrate the ILLL beyond the QL and related observables. We further generalize it to 3D Dirac materials. It will be helpful to understand the unexpected fine structures in conductivity, magnetization, and thermoelectric properties in extremely strong magnetic fields.

TABLE I. The comparison between the oscillation due to the ILLL beyond the QL and the usual SdHO. B is the magnetic field. E_F is the Fermi energy.

	Shubnikov-de Haas	ILLL
Quantum limit	Before	Beyond
B -dependence	Periodic in $1/B$	Periodic in B
Frequency	depends on E_F	does not depend on E_F

* Corresponding author: luhz@sustech.edu.cn

2D graphene-like model – In order to illustrate the ILL, we consider a 4×4 graphene-type model in a z -direction magnetic field B

$$H_{2D} = v \left[\left(k_x + \frac{yeB}{\hbar} \right) \tau_x + k_y \tau_y \right] \otimes \mathbb{1}_2 + \frac{g\mu_B B}{2} \mathbb{1}_2 \otimes \sigma_z, \quad (1)$$

where v is the velocity, k_x, k_y are the wave vectors, y is the position operator, the Pauli matrices (τ_x, τ_y) and σ_z stand for the x, y -direction pseudospin and z -direction real spin, respectively, $\mathbb{1}_2$ is the 2×2 unit matrix, and the last term is the Zeeman splitting with the effective g factor and Bohr magneton μ_B . The cyclotron motion driven by B quantizes the energy spectrum of the pseudospin part into the Landau levels, while the real-spin part takes the Zeeman splitting. The energy spectrum can be found as

$$E_{\nu\lambda s} = \lambda \left(v \sqrt{\frac{2\nu e}{\hbar}} \sqrt{B} + s \frac{g\mu_B}{2} B \right), \quad (2)$$

for Landau indices $\nu = 1, 2, 3, \dots$ and $\lambda, s = \pm 1$; and

$$E_{0\pm} = \pm \frac{g\mu_B}{2} B, \quad (3)$$

for $\nu = 0$. Because of the Dirac nature of the pseudospin part, the energies of the Landau levels scale with \sqrt{B} [29]. The Zeeman splitting, on the other hand, is linear in B . Figure 1 (a) shows the energies of the Landau levels as functions of the magnetic field. There are two distinct features compared to usual cases. First, beyond a critical magnetic field (marked as B_c), the $\nu = 0$ Landau levels $E_{0\pm}$ are no longer the lowest in energy (closest to zero energy). Instead, $E_{1\lambda-}$ become the lowest, then $E_{2\lambda-}$, $E_{3\lambda-}$, ... become the lowest one by one with increasing magnetic field. We refer to this as the inversion of the lowest Landau level, which arises because the linear- B Zeeman splitting overwhelms the \sqrt{B} Landau-level energies. The critical magnetic field required to inverse $E_{0\lambda}$ and $E_{1\lambda-}$ can be found as

$$B_c = \frac{e}{\hbar} \frac{2v^2}{g^2 \mu_B^2}. \quad (4)$$

Above this field is what we referred to as ‘‘beyond the quantum limit’’. This ILL is not observed in graphene, in which $g = 2$ and $v = 1.1 \times 10^6$ m/s (7 eVÅ) so B_c is about 1.2×10^5 T. If $g = 20$, $v = 1.1 \times 10^5$ m/s (0.7 eVÅ), this critical field can be greatly reduced to 12 T, which is accessible to high-magnetic field laboratories. The second feature is that for $\nu \geq 1$ the energies $E_{\nu\lambda-}$ cross when the first term is equal to the second term in Eq. (2).

Fermi energy oscillation beyond the QL – For samples with a large density, the fixed electron density case could be used in most solids. Since the solid is always charge neutral and the current flowing into the sample is in balance with the one flowing out it, the total electron density is a constant [30]. If the samples with small number

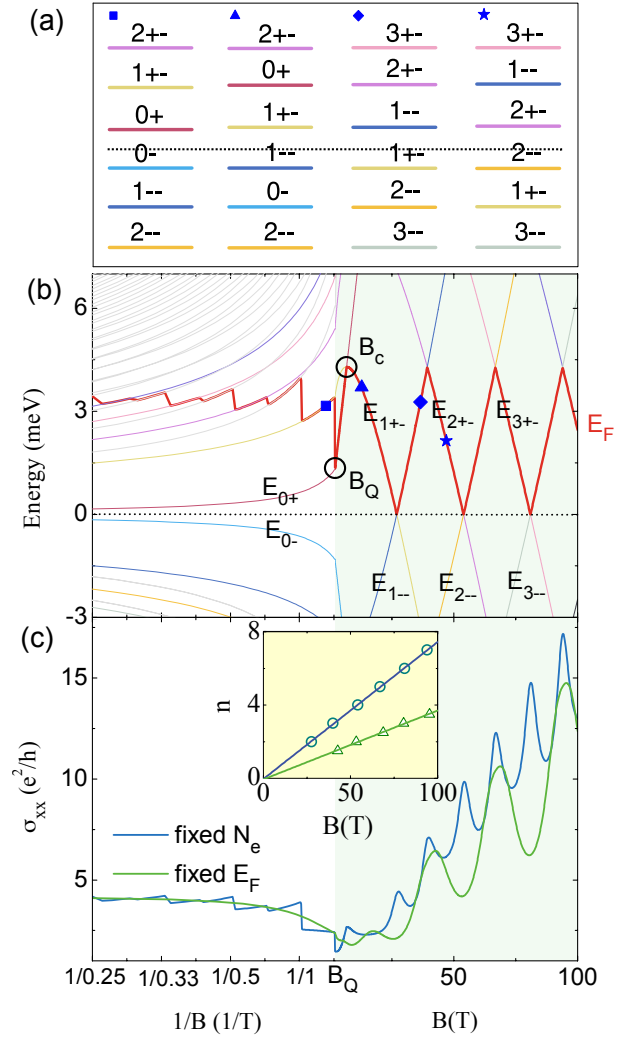


FIG. 1. (Color online) The quantum oscillations beyond the QL (green shadow) induced by the ILL for the 2D graphene-like model in Eq. (1). (a) The energies of the Landau levels at magnetic fields marked by ■, ▲, ◆, and ★ in (b). The dash line indicates the location of the zero energy. (b) The Landau levels and Fermi energy E_F (red) as functions of B for a fixed electron density N_e . ○ mark the critical fields where E_F is moving to E_{0+} (B_Q , the QL) and from E_{0+} to E_{1+-} (B_c), respectively. (c) The conductivity σ_{xx} as a function of the magnetic field for a fixed N_e (blue) or a fixed zero-field Fermi energy E_F^0 (green). Before entering the QL (left side of B_Q), there is the usual SdHO. The inset shows the peaks or dips positions versus the Landau index beyond the QL for fixed density (circle) and Fermi energy (triangle). The parameters are $v = 0.6$ eVÅ, $g = 22$, $N_e = 5 \times 10^{10}$ cm $^{-2}$, and the broadening of levels $\Gamma = 0.002$ eV.

of electrons contact to the metallic reservoirs, the most likely fixed one is the Fermi energy. For the former case, the Fermi energy E_F needs to be determined by how a fixed electron density N_e occupies the Landau levels [24],

according to

$$N_e = \frac{eB}{2\pi\hbar} \left[n_F(E_{0+}) + \sum_{\nu,\lambda,s}^{E_{\nu\lambda s} > 0} n_F(E_{\nu\lambda s}) \right]. \quad (5)$$

Here $n_F(x) = [\exp((x - E_F)/k_B T) + 1]^{-1}$ is the Fermi distribution function. Figure 1 (b) shows the calculated Fermi energy as a function of the magnetic field for a fixed N_e . Before entering the QL (the white regime), the Fermi energy is almost unchanged with increasing magnetic field. For usual cases, the Landau levels remain in the same order, the Fermi energy will be pushed down onto the Landau level with the lowest index (conventionally denoted as 0th) and stays there at higher magnetic fields, which is the QL. In contrast, here the ILL and periodic crossing of $E_{\nu\lambda-}$ lead to the strong oscillation of the Fermi energy beyond the QL. E_F shows dips where the energies $E_{\nu\lambda-}$ ($\nu \geq 1$) cross. The period of the oscillation of E_F is found as $B_T = 4B_c$.

Conductivity oscillation beyond the QL – This oscillation beyond the QL can be measured in the conductivity. We calculate the longitudinal conductivity σ_{xx} with the help of the Kubo formula [31] $\sigma_{xx} = -(\hbar e^2/2\pi V) \int d\varepsilon (\partial n_F/\partial \varepsilon) \text{Tr}(v_x G^R v_x G^A)$, where V is the area for 2D or the volume for 3D system, $G^{R/A}$ are the retarded and advanced Green's functions, respectively, and v_x is the x -direction velocity operator.

Figure 1 (c) shows the longitudinal conductivities for fixed electron density N_e and zero-field Fermi energy E_F^0 , respectively. Before entering the QL, there is the usual SdHO of the conductivity (the white regime), periodic in $1/B$. More importantly, a much stronger oscillation appears beyond the QL (the green shadow) for both two cases. The oscillation beyond the QL is periodic in the magnetic field B , not in $1/B$ as the usual SdHO is. The period for fixed E_F^0 is $B_T = 4B_c$. However, for fixed density, the frequency of conductivity doubles compared with that of the Fermi energy, because the Dirac fermion is massless. If the Dirac fermion has no mass, the Landau levels $E_{\nu\pm-}$ can cross, so the Fermi energy can drop to zero and cross the negative level $E_{\nu--}$ (see Fig. 1 (b)). As a result, conductivity peaks also occur at the zeros of the Fermi energy. The period of the conductivity beyond the QL can thus be found as $B_T = 2B_c$. The period of the oscillation beyond the QL does not depend on the Fermi energy, quite different from the usual SdHO [32, 33]. It only depends on the ratio of the Fermi velocity and the g factor, which determines the ILL. This novel linear- B oscillation gives a zero phase shift in the $n - B$ Landau fan diagram if one assigns integer numbers to the peaks or dips of conductivity, as shown in the inset of Fig. 1 (c). This is valid for both fixed Fermi energy and electron density. Previously, linear- B oscillations are usually due to the quantum coherent transport such as Aharonov-Bohm effect or Altshuler-Aronov-Spivak effect. Here we demonstrate a new linear- B oscillation.

All these feature could be understood from the analytical results of the density of states before and beyond the

QL written as [31]

$$\varrho(E_F \gg E_{0+}) \simeq \frac{E_F}{\pi v^2} + A_1 \cos\left(2\pi \frac{\hbar E_F^2}{2v^2 eB}\right), \quad (6)$$

$$\varrho(E_F \ll E_{0+}) \simeq \frac{g\mu_B B}{2\pi v^2} + A_2 \cos\left(2\pi \frac{\hbar g^2 \mu_B^2 B}{8ev^2}\right). \quad (7)$$

Here amplitudes $A_1 = \frac{2E_F}{\pi v^2} \exp(-\frac{2\pi\hbar E_F \Gamma}{v^2 eB})$ and $A_2 = \frac{g\mu_B B}{\pi v^2} \exp(-\frac{\pi\hbar g\mu_B \Gamma}{ev^2})$. For $E_F \gg E_{0+}$ (before the QL), the density of states oscillates inversely with the field as the usual SdHO. However, beyond the QL ($E_F \ll E_{0+}$), the density of states oscillates with the magnetic field having a period $B_T = 4B_c$. Further, the phase shift of this B -oscillation equals zero for both two cases. The whole density of states beyond the QL $\varrho(E_F \ll E_{0+})$ is independent of the Fermi energy. The amplitude of the usual oscillation before the QL increases with the field due to the increase of the Dingle factor. However, the amplitude beyond the QL is even larger since the ratio

$$\frac{A_2}{A_1} = \frac{E_{0+}}{E_F} e^{-2\pi\hbar(E_{0+}-E_F)\Gamma/(v^2 eB)} > 1, \quad (8)$$

because of the factor $E_{0+} \gg E_F$ and small broadening Γ , $e^{-2\pi\hbar(E_{0+}-E_F)\Gamma/(v^2 eB)} \sim 1$.

Oscillation due to the inversion of the lowest Landau band beyond the QL in 3D – The above discussion in 2D system can be generalized to 3D case. In a z -direction magnetic field B , we use a $\mathbf{k} \cdot \mathbf{p}$ Hamiltonian [34]

$$H = v \left[\left(k_x + \frac{yeB}{\hbar} \right) \tau_x \otimes \sigma_z + k_y \tau_y \otimes \mathbb{1}_2 + k_z \tau_x \otimes \sigma_x \right] + m\tau_z \otimes \mathbb{1}_2 + \delta \mathbb{1}_2 \otimes \sigma_z, \quad (9)$$

where v and m are the Fermi velocity and mass, respectively, and $\delta = g\mu_B B/2$ is the Zeeman field. This model can describe the low-energy spectrum for a variety of Dirac materials, from semimetals to insulators. The energy spectrum is found as

$$E_{\nu\lambda s} = \lambda \sqrt{\left(\sqrt{\nu\omega^2 + m^2} + s\delta \right)^2 + v^2 k_z^2}, \quad (10)$$

for $\nu \geq 1$; and

$$E_{0\lambda} = \lambda \sqrt{(m - \delta)^2 + v^2 k_z^2}, \quad (11)$$

for $\nu = 0$. Here $\omega = v\sqrt{2eB/\hbar}$. Instead of the Landau levels, we have the bands of Landau levels that disperse with k_z , because the k_z along the direction of magnetic field is a good quantum number. Each time $\delta = \sqrt{\nu\omega^2 + m^2}$, $E_{\nu+-}$ crosses with $E_{\nu--}$. Without loss of generality, we assume the carrier is electron, the Fermi energy E_F can be determined from the 3D electron density for fixed density

$$N_e = \frac{eB}{2\pi\hbar} \sum_{k_z} \left[n_F(E_{0+}) + \sum_{\nu,s} n_F(E_{\nu+s}) \right]. \quad (12)$$

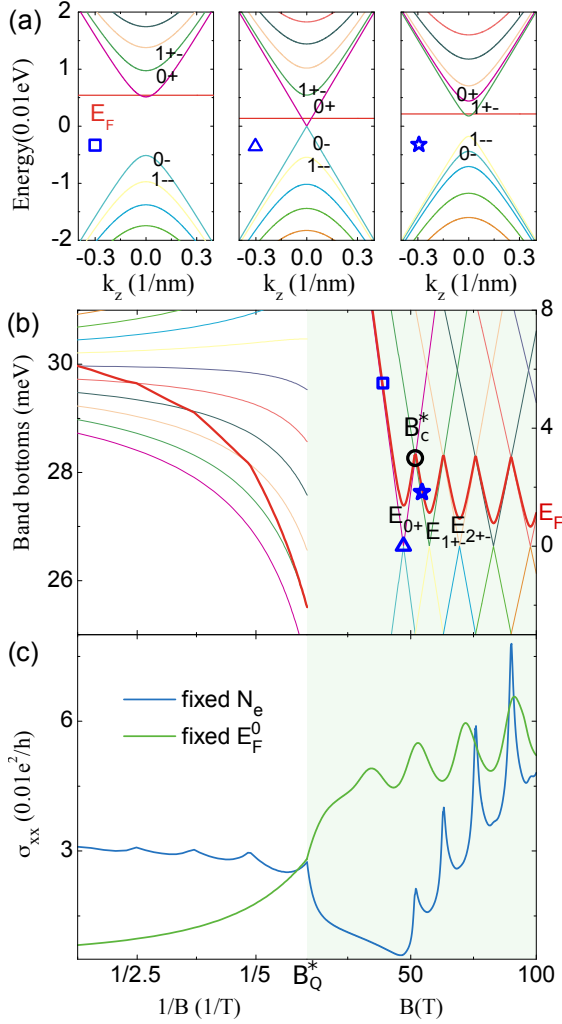


FIG. 2. (Color online) The quantum oscillations beyond the QL (green shadow) induced by the inversion of the lowest Landau band for the 3D Dirac model in Eq. (9). (a) The 1D bands (disperse with k_z) of the Landau levels at magnetic fields marked by \square , \triangle , and \star in (b). (b) The band bottoms of E_{0+} , E_{1+-} , \dots and the Fermi energy E_F (red solid) as functions of B for a fixed density N_e . \circ marks the critical field B_c^* where E_F is moving from E_{0+} to E_{1+-} . (c) The conductivity σ_{xx} as a function of the magnetic field for a fixed N_e or a fixed zero-field Fermi energy E_F^0 . σ_{xx} for a fixed E_F^0 has been divided by 7 for display. The QL critical magnetic field B_Q^* is 8.8 T. The SdHO is on the left with $1/B$ as the horizontal axis. The parameters are $v = 0.5 \text{ eV}\text{\AA}$, $m = 0.03 \text{ eV}$, $g = 22$ [34–36], $N_e = 1 \times 10^{17} \text{ cm}^{-3}$, and $\Gamma = 0.001 \text{ eV}$.

When the Zeeman splitting δ overwhelms the Landau energies $\sqrt{\nu\omega^2 + m^2}$, the inversion of the lowest Landau band arises, leading to the oscillation of Fermi energy and conductivity [Fig. 2 (b) and (c)] beyond the QL. The critical magnetic field of the inversion can be found as

$$B_c^* = \frac{e}{\hbar} \frac{2v^2}{g^2\mu_B^2} + \frac{2m}{g\mu_B}. \quad (13)$$

At the magnetic field where the lowest Landau band inverts, the Fermi energy for fixed electron density indicates a dip, as shown in Fig. 2 (b). The amplitude of the oscillation beyond the QL is also much larger than that of the usual SdHO. For quantities sensitive to the Fermi energy, such as the thermal power, this oscillation is even more remarkable. For a fixed Fermi energy, there is also a oscillation of conductivity with larger amplitude comparing to the SdHO (the green line in Fig. 2 (b)), but the amplitude and peak positions are quite different from those with a fixed N_e . The 3D oscillation beyond the QL is also periodic in B . With a large g or small v , the spacing between the oscillation peaks can be found as $B_T \approx 4B_c$ just as the Fermi energy of fixed N_e for small gap m .

Experimental implications and discussions – Distinct from other unexpected fine structures [13–24] at extremely strong magnetic fields, our work proposes a new possible phenomenon. This B -oscillation is observable in Dirac materials where momentum is coupled only to pseudospin, if the magnetic field is large enough. It can be observed at an accessible magnetic field in materials with a small Fermi velocity v or large g factor. To observe it at a magnetic field of 40 T, the ratio g/v has to be about $200 / \text{eV nm}$. In artificial systems that can be described by the Dirac models, such as the InAs/GaSb asymmetric quantum well and GaSb/InAs/GaSb symmetric quantum well, the electrically-tuned Fermi velocity [37, 38] varies from 0.07 to 0.3 $\text{eV}\text{\AA}$ [39, 40] and the g factor is about 10 [41], so the ratio $g/v \in [330, 1400] \text{ eV}^{-1}\text{nm}^{-1}$, suggesting that these systems are better candidates for the oscillation beyond the QL. Moreover, the critical magnetic field for the novel inversion can be reduced by doping magnetic impurities, which effectively enhances the Zeeman g factor. Also, considering the continuous growth of the largest magnetic field generated in laboratories [42, 43], this novel oscillation may be observed in a near future.

Here both two Dirac models contain only one Fermi pocket. For a system having N pseudospin Dirac pockets with relatively small Fermi velocities v_i and large g factors g_i ($i = 1, \dots, N$), if the distances among these pockets are small enough, the magnetic breakdown [44–47] due to the tunneling between pockets may occur. Beyond the QL of all pockets, this novel B -type oscillation will have a period of $B_T = (4e/\hbar)[\sum_i (g_i^2 \mu_B^2 / v_i^2)]^{-1}$ in 2D and $B_T = (8e/\hbar)[\sum_i (g_i^2 \mu_B^2 / v_i^2)]^{-1}$ in 3D. If only a portion of pockets are beyond the QL, the oscillation will be between B -type and $1/B$ -type.

This B -oscillation can also happen in the ballistic regime, where the conductance has nothing to do with disorder but depends on the density of states [48], so can directly probe the ILL. Here we only consider the oscillation of the conductivity, other physical quantities such as magnetic susceptibility and magnetization in de Haas-van Alphen effect can also exhibit this novel quantum oscillation, up to some phase shifts. It should be noted that the mechanism of the ILL is completely different from the Zeeman splitting in usual systems [36, 49–52]. Al-

though in usual systems the Landau level inversion may also happen for higher index levels with large Zeeman splitting, the lowest one is always the zeroth level. Therefore, this oscillation does not occur in traditional semiconductors with parabolic dispersion and real-spin Dirac materials. In some cases of pseudospin Dirac materials, the magnetic field may lift negative energy Landau levels up to the Fermi energy to give rise to oscillations (Fig. 1 (a)). In other cases, the oscillation beyond the QL could have nothing to do with the negative-energy Landau levels (Fig. 2 (a)), solely as a result of the competition between orbital pseudospin and Zeeman real-spin degrees of freedom of one type of carriers. This novel phenomenon may also exist widely in topological materials with both real spin and pseudospin degrees of freedom, where the energy spectrum linearly depends on the momentum near the contacting points between conduction and valence bands.

We discuss some physical effects that may spoil this oscillation. The fractional quantum Hall effect may happen when the last Landau level is occupied in conventional two-dimensional electron gases, because of strong Coulomb interactions. For the present case, the electron-electron interaction could also be significant. However, the last level and fractional filling is not well defined as a result of the level inversion. The interaction may influence the oscillation in other ways. Other physical phe-

nomena involving spin degree of freedom may also affect this oscillation. If the energy scales relating to these effects are smaller than the Zeeman splitting, the profile of the oscillation is supposed to be observable. The unavoidable level repulsion in real systems may open a gap near the level crossing. However, the ILL still exists for small electron density. Therefore, the occupied lowest level still changes with the change of the field, then the B -oscillation of the Fermi energy or the conductivity is also expected to be observed.

Acknowledgments – This work was supported by the National Natural Science Foundation of China (11534001, 11974249, and 11925402), the Strategic Priority Research Program of Chinese Academy of Sciences (Grant No. XDB28000000), Guangdong Innovative and Entrepreneurial Research Team Program (2016ZT06D348), the National Key R & D Program (2016YFA0301700), the Natural Science Foundation of Shanghai (Grant No. 19ZR1437300), Shenzhen High-level Special Fund (No. G02206304, G02206404), and the Science, Technology and Innovation Commission of Shenzhen Municipality (ZDSYS20170303165926217, JCYJ20170412152620376, KYTDPT20181011104202253). The numerical calculations were supported by Center for Computational Science and Engineering of Southern University of Science and Technology.

-
- [1] X. Wan, A. M. Turner, A. Vishwanath, and S. Y. Savrasov, “Topological semimetal and Fermi-arc surface states in the electronic structure of pyrochlore iridates”, *Phys. Rev. B* **83**, 205101 (2011).
- [2] K. Y. Yang, Y. M. Lu, and Y. Ran, “Quantum Hall effects in a Weyl semimetal: Possible application in pyrochlore iridates”, *Phys. Rev. B* **84**, 075129 (2011).
- [3] A. A. Burkov and L. Balents, “Weyl semimetal in a topological insulator multilayer”, *Phys. Rev. Lett.* **107**, 127205 (2011).
- [4] G. Xu, H. M. Weng, Z. J. Wang, X. Dai, and Z. Fang, “Chern semimetal and the quantized anomalous Hall effect in HgCr_2Se_4 ”, *Phys. Rev. Lett.* **107**, 186806 (2011).
- [5] P. Delplace, J. Li, and D. Carpentier, “Topological Weyl semi-metal from a lattice model”, *EPL* **97**, 67004 (2012).
- [6] J.-H. Jiang, “Tunable topological Weyl semimetal from simple-cubic lattices with staggered fluxes”, *Phys. Rev. A* **85**, 033640 (2012).
- [7] S. M. Young, S. Zaheer, J. C. Y. Teo, C. L. Kane, E. J. Mele, and A. M. Rappe, “Dirac semimetal in three dimensions”, *Phys. Rev. Lett.* **108**, 140405 (2012).
- [8] Z. Wang, Y. Sun, X. Q. Chen, C. Franchini, G. Xu, H. Weng, X. Dai, and Z. Fang, “Dirac semimetal and topological phase transitions in A_3Bi ($\text{A} = \text{Na}, \text{K}, \text{Rb}$)”, *Phys. Rev. B* **85**, 195320 (2012).
- [9] B. Singh, A. Sharma, H. Lin, M. Z. Hasan, R. Prasad, and A. Bansil, “Topological electronic structure and Weyl semimetal in the TlBiSe_2 class of semiconductors”, *Phys. Rev. B* **86**, 115208 (2012).
- [10] Z. Wang, H. Weng, Q. Wu, X. Dai, and Z. Fang, “Three-dimensional Dirac semimetal and quantum transport in Cd_3As_2 ”, *Phys. Rev. B* **88**, 125427 (2013).
- [11] J. Liu and D. Vanderbilt, “Weyl semimetals from noncentrosymmetric topological insulators”, *Phys. Rev. B* **90**, 155316 (2014).
- [12] D. Bulmash, C.-X. Liu, and X.-L. Qi, “Prediction of a Weyl semimetal in HgCdMnTe ”, *Phys. Rev. B* **89**, 081106(R) (2014).
- [13] C.-L. Zhang, S.-Y. Xu, C. M. Wang, Z. Lin, Z. Z. Du, C. Guo, C.-C. Lee, H. Lu, Y. Feng, S.-M. Huang, *et al.*, “Magnetic-tunnelling-induced Weyl node annihilation in TaP”, *Nat. Phys.* **13**, 979 (2017).
- [14] B. J. Ramshaw, K. A. Modic, A. Shekhter, Y. Zhang, E.-A. Kim, P. J. W. Moll, M. D. Bachmann, M. K. Chan, J. B. Betts, F. Balakirev, *et al.*, “Quantum limit transport and destruction of the Weyl nodes in TaAs”, *Nat. Commun.* **9**, 2217 (2018).
- [15] P. Kim, J. H. Ryoo, and C.-H. Park, “Breakdown of the chiral anomaly in Weyl semimetals in a strong magnetic field”, *Phys. Rev. Lett.* **119**, 266401 (2017).
- [16] H. Wang, H. Liu, Y. Li, Y. Liu, J. Wang, J. Liu, J.-Y. Dai, Y. Wang, L. Li, J. Yan, *et al.*, “Discovery of log-periodic oscillations in ultraquantum topological materials”, *Sci. Adv.* **4**, eaau5096 (2018).
- [17] Y. Chen, H.-Z. Lu, and X. C. Xie, “Forbidden backscattering and resistance dip in the quantum limit as a signature for topological insulators”, *Phys. Rev. Lett.* **121**, 036602 (2018).
- [18] B. A. Assaf, T. Phuphachong, E. Kampert, V. V. Volobuev, P. S. Mandal, J. Sánchez-Barriga, O. Rader,

- G. Bauer, G. Springholz, L. A. de Vaulchier, *et al.*, “Negative longitudinal magnetoresistance from the anomalous $N = 0$ Landau level in topological materials”, *Phys. Rev. Lett.* **119**, 106602 (2017).
- [19] J. L. Zhang, C. M. Wang, C. Y. Guo, X. D. Zhu, Y. Zhang, J. Y. Yang, Y. Q. Wang, Z. Qu, L. Pi, H.-Z. Lu, *et al.*, “Anomalous thermoelectric effects of ZrTe_5 in and beyond the quantum limit”, *Phys. Rev. Lett.* **123**, 196602 (2019).
- [20] V. Kozii, B. Skinner, and L. Fu, “Thermoelectric Hall conductivity and figure of merit in Dirac/Weyl materials”, *Phys. Rev. B* **99**, 155123 (2019).
- [21] W. Zhang, P. Wang, B. Skinner, R. Bi, V. Kozii, C.-W. Cho, R. Zhong, J. Schneeloch, D. Yu, G. Gu, *et al.*, “Observation of a thermoelectric Hall plateau in the extreme quantum limit”, *Nat. Commun.* **11**, 1046 (2020).
- [22] F. Han, N. Andrejevic, T. Nguyen, V. Kozii, Q. Nguyen, Z. Ding, R. Pablo-Pedro, S. Parjan, B. Skinner, A. Alatas, *et al.*, “Discovery of giant, non-saturating thermopower in topological semimetal at quantum limit”, [arXiv:1904.03179](https://arxiv.org/abs/1904.03179) (2019).
- [23] P. J. W. Moll, A. C. Potter, N. L. Nair, B. Ramshaw, K. Modic, S. Riggs, B. Zeng, N. J. Ghimire, E. D. Bauer, R. Kealhofer, *et al.*, “Magnetic torque anomaly in the quantum limit of Weyl semimetals”, *Nat. Commun.* **7**, 12492 (2016).
- [24] C.-L. Zhang, C. M. Wang, Z. Yuan, X. Xu, G. Wang, C.-C. Lee, L. Pi, C. Xi, H. Lin, N. Harrison, *et al.*, “Non-saturating quantum magnetization in Weyl semimetal TaAs ”, *Nat. Commun.* **10**, 1028 (2019).
- [25] M. König, S. Wiedmann, C. Brüne, A. Roth, H. Buhmann, L. W. Molenkamp, X.-L. Qi, and S.-C. Zhang, “Quantum spin Hall insulator state in HgTe quantum wells”, *Science* **318**, 766 (2007).
- [26] S. B. Zhang, H. Z. Lu, and S. Q. Shen, “Edge states and integer quantum Hall effect in topological insulator thin films”, *Sci. Rep.* **5**, 13277 (2015).
- [27] Y. A. Bychkov and E. I. Rashba, “Oscillatory effects and the magnetic susceptibility of carriers in inversion layers”, *J. Phys. C: Solid State Phys.* **17**, 6039 (1984).
- [28] X. F. Wang and P. Vasilopoulos, “Magnetotransport in a two-dimensional electron gas in the presence of spin-orbit interaction”, *Phys. Rev. B* **67**, 085313 (2003).
- [29] A. H. Castro Neto, F. Guinea, N. M. R. Peres, K. S. Novoselov, and A. K. Geim, “The electronic properties of graphene”, *Rev. Mod. Phys.* **81**, 109 (2009).
- [30] G. D. Mahan, *Many-Particle Physics* (Plenum Press, 1990).
- [31] See Supplemental Materials for the detailed calculations.
- [32] C. M. Wang, H.-Z. Lu, and S.-Q. Shen, “Anomalous phase shift of quantum oscillations in 3D topological semimetals”, *Phys. Rev. Lett.* **117**, 077201 (2016).
- [33] C. Li, C. M. Wang, B. Wan, X. Wan, H.-Z. Lu, and X. C. Xie, “Rules for phase shifts of quantum oscillations in topological nodal-line semimetals”, *Phys. Rev. Lett.* **120**, 146602 (2018).
- [34] R. Y. Chen, Z. G. Chen, X.-Y. Song, J. A. Schneeloch, G. D. Gu, F. Wang, and N. L. Wang, “Magnetoinfrared spectroscopy of Landau levels and Zeeman splitting of three-dimensional massless Dirac fermions in ZrTe_5 ”, *Phys. Rev. Lett.* **115**, 176404 (2015).
- [35] H. Weng, X. Dai, and Z. Fang, “Transition-metal pentatelluride ZrTe_5 and HfTe_5 : A paradigm for large-gap quantum spin Hall insulators”, *Phys. Rev. X* **4**, 011002 (2014).
- [36] Y. Liu, X. Yuan, C. Zhang, Z. Jin, A. Narayan, C. Luo, Z. Chen, L. Yang, J. Zou, X. Wu, *et al.*, “Zeeman splitting and dynamical mass generation in Dirac semimetal ZrTe_5 ”, *Nat. Commun.* **7**, 12516 (2016).
- [37] S. S. Krishtopenko and F. Teppe, “Quantum spin Hall insulator with a large bandgap, Dirac fermions, and bilayer graphene analog”, *Sci. Adv.* **4**, eaap7529 (2018).
- [38] T. Campos, M. A. T. Sandoval, L. Diago-Cisneros, and G. M. Sipahi, “Electrical tuning of helical edge states in topological multilayers”, *J. Phys.: Condens. Matter* **31**, 495501 (2019).
- [39] I. Knez, C. T. Rettner, S.-H. Yang, S. S. P. Parkin, L. Du, R.-R. Du, and G. Sullivan, “Observation of edge transport in the disordered regime of topologically insulating InAs/GaSb quantum wells”, *Phys. Rev. Lett.* **112**, 026602 (2014).
- [40] T. Li, P. Wang, H. Fu, L. Du, K. A. Schreiber, X. Mu, X. Liu, G. Sullivan, G. A. Csáthy, X. Lin, *et al.*, “Observation of a helical Luttinger liquid in InAs/GaSb quantum spin hall edges”, *Phys. Rev. Lett.* **115**, 136804 (2015).
- [41] X. Mu, G. Sullivan, and R.-R. Du, “Effective g-factors of carriers in inverted InAs/GaSb bilayers”, *Appl. Phys. Lett.* **108**, 012101 (2016).
- [42] D. Nakamura, A. Ikeda, H. Sawabe, Y. H. Matsuda, and S. Takeyama, “Record indoor magnetic field of 1200 T generated by electromagnetic flux-compression”, *Rev. Sci. Instrum.* **89**, 095106 (2018).
- [43] D. Nakamura, H. Saito, H. Hibino, K. Asano, and S. Takeyama, “Quantum limit cyclotron resonance in monolayer epitaxial graphene in magnetic fields up to 560 T: The relativistic electron and hole asymmetry”, *Phys. Rev. B* **101**, 115420 (2020).
- [44] M. H. Cohen and L. M. Falicov, “Magnetic breakdown in crystals”, *Phys. Rev. Lett.* **7**, 231 (1961).
- [45] M. G. Priestley, L. M. Falicov, and G. Weisz, “Experimental and theoretical study of magnetic breakdown in magnesium”, *Phys. Rev.* **131**, 617 (1963).
- [46] T. E. O’Brien, M. Diez, and C. W. J. Beenakker, “Magnetic breakdown and Klein tunneling in a type-II Weyl semimetal”, *Phys. Rev. Lett.* **116**, 236401 (2016).
- [47] A. Alexandradinata and L. Glazman, “Geometric phase and orbital moment in quantization rules for magnetic breakdown”, *Phys. Rev. Lett.* **119**, 256601 (2017).
- [48] S. Datta, *Quantum Transport: Atom to Transistor* (Cambridge University Press, 2005).
- [49] J. Cao, S. Liang, C. Zhang, Y. Liu, J. Huang, Z. Jin, Z. G. Chen, Z. Wang, Q. Wang, J. Zhao, *et al.*, “Landau level splitting in Cd_3As_2 under high magnetic fields”, *Nat. Commun.* **6**, 7779 (2015).
- [50] J. Hu, Z. Tang, J. Liu, Y. Zhu, J. Wei, and Z. Mao, “Nearly massless Dirac fermions and strong Zeeman splitting in the nodal-line semimetal ZrSiS probed by de Haas-van Alphen quantum oscillations”, *Phys. Rev. B* **96**, 045127 (2017).
- [51] J. Wang, J. Niu, B. Yan, X. Li, R. Bi, Y. Yao, D. Yu, and X. Wu, “Vanishing quantum oscillations in Dirac semimetal ZrTe_5 ”, *Proc. Natl. Acad. Sci. USA* **115**, 9145 (2018).
- [52] R. Bi, Z. Feng, X. Li, J. Niu, J. Wang, Y. Shi, D. Yu, and X. Wu, “Spin zero and large Landé g-factor in WTe_2 ”, *New J. Phys.* **20**, 063026 (2018).